Removal efficiency of hexavalent chromium from wastewater using starch-stabilized nanoscale zero-valent iron

Hualin Chen, Huajun Xie, Jiangmin Zhou, Yueliang Tao, Yongpu Zhang, Qiansong Zheng and Yufeng Wang

ABSTRACT

In this study, starch-stabilized nanoscale zero-valent iron (S-nZVI) was produced using the liquid-phase reduction method. It was used to remove chromium from wastewater, and compared to a commercial nanoscale zero-valent iron (C-nZVI). Both nZVIs were characterized by scanning electron microscopy (SEM), X-ray diffraction (XRD) and X-ray photoelectron spectroscopy (XPS). The characterization results showed that S-nZVI had smaller particles and a more uniform particle size distribution than C-nZVI. Both nZVIs showed a core-shell structure with the Fe^0 core prominently surrounded by less iron oxides of Fe^{2+} and Fe^{3+}. The optimal application methods to remove Cr(VI) from wastewater were also explored. The results showed that both the removal efficiencies of total Cr and Cr(VI) increased with increases in the addition of nZVIs, while the removal efficiencies of total Cr and Cr(VI) by S-nZVI were clearly higher than that of C-nZVI, especially in a low pH range (pH = 1.0–6.0). This research indicated that starch-stabilized nanoscale zero-valent iron is a valuable material to remove heavy metals from wastewater due to its stability and high reactivity.

Key words | chromium-containing wastewater, iron, nanoscale, starch

Hualin Chen (corresponding author)
Huajun Xie
Jiangmin Zhou
Yueliang Tao
Yongpu Zhang
Qiansong Zheng
College of Life and Environmental Science,
Wenzhou University,
Wenzhou 325035,
China
E-mail: *hualin2100@126.com*

Yufeng Wang
Zhejiang Zone-King Environmental Sci & Tech Co., Ltd,
Hangzhou 310014,
China

INTRODUCTION

Chromium (Cr) is one of the toxic metals in widespread use, and can be found in the atmosphere, water and soil (Mihaileanu *et al.* 2019). Chromium is discharged into the environment from activities such as mineral extraction, electroplating, steel and alloy production, leather tanning, and pigment and chemical manufacturing. According to the Annual Environmental Statistics of China in 2017, the total Cr discharged by industrial activities in 2015 reached 104.4 tonnes, including 23.5 tonnes Cr(VI). Chromium has two stable oxidation forms, Cr(III) and Cr(VI). Cr(III) is less toxic and can form complexes with hydroxides at typical water pH to form $Cr(OH)_3$, making it immobile. Cr(VI) is highly soluble and extremely mobile in the hydrosphere. It is approximately 300 times more toxic than Cr(III) and is categorized as carcinogenic and mutagenic (Nickens *et al.* 2010). Hence, excess chromium in the environment is harmful to ecosystems, and may inhibit plant and microorganism growth and metabolism, as well as threatening human health (Chen *et al.* 2014). Therefore, strategies need to be applied to remediate chromium-contaminated water and soil.

Many technologies have been developed to treat wastewater containing chromium from industrial effluent, including chemical precipitation, adsorption, electrolysis, membrane separation, and photocatalysis. Among these technologies, chemical precipitation is most commonly used to removal chromium from wastewater, despite the shortcomings of a high sludge yield and the difficulties of sludge disposal. Electrolysis, photocatalysis and membrane separation are feasible options to remove chromium from wastewater. However, these technologies are hampered by the high costs.

Nanoparticles of iron (Fe) oxides, especially zero-valent iron (nZVI) are environmentally friendly and useful materials characterized by small particle size, high surface area, strong reducing ability, and fast reaction (Zhao *et al.* 2016). Therefore, in recent years, nZVI has been widely used in the field of remediation of water bodies (Broujeni *et al.* 2018; Zhu *et al.* 2018). Many researchers have reported that nZVI can be used to remove Cr, Cd, Zn, Pb, and other heavy metals, and also organic pollutants from wastewater

doi: 10.2166/wst.2019.358

(Li *et al.* 2015; Ambika *et al.* 2016). A study by Wang *et al.* (2014) revealed that nZVI successfully reduced graphite oxide composite and removed As(III) and As(V) from aqueous solution, with capacities of 35.83 and 29.04 mg g^{-1}, respectively. Klimkova *et al.* (2011) reported that nZVI was effective for chromium removal from acid mine water. For chromium removal by nZVI, the process normally involves the reduction of Cr(VI) to Cr(III) and eventual precipitation of Fe/Cr-OH compounds (Gheju & Balcu 2011). The addition of one gram of nZVI reduced 84.4–109.3 mg Cr(VI) and 69.3–72.7 mg Cr(VI), respectively in the contaminated groundwater (43 mg Cr-VI L^{-1}) and residues from chrome processing (3,280 mg Cr-VI kg^{-1}) (Cao & Zhang 2006).

The nZVI used in the reduction of Cr(VI) to Cr(III) covers a wide range of materials. Gheju & Balcu (2011), have described them as (1) commercial and reagent grade, (2) laboratory synthesized and (3) scrap iron. Commercially-available nZVI, referred to as 'granular iron', 'iron filings', 'iron chips', 'iron shavings', is made from ground scrap iron, cast iron or steel annealed under an oxidizing atmosphere. Laboratory synthesized nZVI is produced by the borohydride reduction method of ferric or ferrous iron. Scrap iron is recycled iron-containing materials such as steel. Evidence from wastewater treatments and batch experiments with soils show the promise of using iron nanoparticles to reduce chromate mobility in the environment.

However, nZVI has some shortcomings, such as poor air stability, difficulty of preservation, and easy reunion (Kong *et al.* 2016). Jabeen *et al.* (2013) reported that an nZVI composite removed Pb(II) ions with an adsorption capacity of 181.04 mg g^{-1}. The authors used non-stabilized nZVI to form the nZVI–graphene composite, which could quickly be oxidized due to its strong oxidizing ability and the lack of a coating to prevent its oxidation. Hence, it is better to use a coated nZVI so that it does not rapidly oxidize and will therefore have a higher reaction capacity (Wijesekara *et al.* 2014).

Starch is a nontoxic, biodegradable, and inexpensive substance that can be used as an effective dispersant for iron nanoparticles. Starch is a polymer of glucose with a complicated chain structure, which can be the adherence site for nanoparticles and can prevent the reunion of nZVI (Kumarathilaka *et al.* 2016). Although a few studies have investigated heavy metal removal efficiency from wastewater by nZVI nanoparticles, there is little available information on Cr(VI) removal by stabilized nZVI nanoparticles. For this reason, starch-stabilized nanoscale zero-valent iron (S-nZVI) was synthesized in this research to improve the stability and dispersibility in an aqueous medium. The overarching goal of this work was to evaluate the performance of S-nZVI for chromium removal from wastewater. Scanning electron microscopy (SEM), X-ray photoelectron spectroscopy (XPS) and X-ray powder diffraction (XRD) analyses were used to characterize the microstructure of nZVI to reveal the governing mechanisms of the reduction and adsorption processes.

MATERIALS AND METHODS

Materials

In this study, iron (II) sulfate ($FeSO_4$), absolute ethanol and hydrogen chloride were obtained from Sigma–Aldrich and used without further purification. Standard chromium solutions of different concentrations were prepared by dilution of 100 mg Cr(VI) L^{-1} stock solution prepared from analytical grade K_2CrO_4 with deionized water (MilliQ) and the initial pH was adjusted using nitric acid and sodium hydroxide.

The wastewater in this research was sampled from an electroplating sewage treatment plant located at Yueqing electroplating base in Wenzhou City, Zhejiang Province, China. The wastewater from different electroplating plants is collected separately as copper-containing, chromium-containing, nickel-containing, cyanide-containing, pickling, and comprehensive wastewater. The five types of wastewater are pumped into the sewage treatment plant to be treated using different processes according to the wastewater properties. We collected chromium-containing wastewater for our research, and the basic properties of the wastewater are presented in Table 1.

Synthesis of S-nZVI

In this study, S-nZVI was synthesized using the conventional liquid-phase method by reducing the ferric ion with sodium borohydride ($NaBH_4$) with some modifications. The synthesis was conducted in a 1.0-L flask containing 100 mL 0.4 mol L^{-1} $FeSO_4$, 2 g corn starch, and 100 mL ethanol. The flask was then stirred in an ultrasonic bath for 30 min,

Table 1 | The basic chemical properties of the chromium-containing wastewater from the electroplating sewage treatment plant (mg L^{-1}, except pH)

pH	Total Cr	Cr(VI)	Cu	Zn	Pb	Cd
1.98	712.2	510.81	138.1	318.4	5.76	0.96

thereafter $NaBH_4$ (0.4 mol L^{-1}) was added until the reaction finished. A magnet was applied to facilitate nZVI precipitation. All the procedures were conducted under a nitrogen gas flow to avoid oxygen dissolving in the aqueous phase. The precipitated S-nZVI slurries were transferred to centrifuge tubes and immediately sealed with parafilm inside the chamber. Thereafter, the nZVI particles were separated by centrifugation at $2{,}500 \times g$ for 10 min, after which the supernatant was discarded, and the residue in the centrifuge tubes was washed using absolute ethanol. This procedure was repeated three times. After the final centrifugation, the composites were freeze dried, and prepared composites were stored at <4 °C in sealed bags. The procedure was repeated numerous times to collect sufficient nanocomposites for the study.

A commercially available nanoscale zero-valent iron (C-nZVI) (Fisher, 100 mesh) was used in this study as a benchmark material.

Characterization of nZVIs

The structure and composition of the nZVIs were characterized by SEM (SEM-EDX, JEOL JSM-7500 operated at 20 kV), XPS (XPS, ESCALAB 250) and XRD (XRD, Rigaku Dmax III with Cu K_α radiation).

SEM: Samples were dried at room temperature and sprinkled onto adhesive carbon tapes supported on metallic stubs and then coated with carbon. Particle size was determined from SEM images using Nano Measurer 1.2.5 software.

XPS: An aluminum rotating anode serves as the X-ray source and generates a KR X-ray beam (1,486.6 eV). The X-ray beam is monochromatized using seven crystals mounted on three Rowland circles. The energy is analyzed using a high-resolution 300 mm mean radius hemispherical electrostatic analyzer and detected by a multichannel plate-CCD camera. The binding energies of the photoelectrons are correlated by the aliphatic hydrocarbon C(1 s) peak at 284.6 eV.

XRD: The XRD patterns were recorded using Cu K_α ($\lambda = 1.54$ Å) radiation on a Rigaku D/max-IIIB diffractometer operating at 40 kV and 20 mA between 10° and 80° (2θ) at a step size of 0.02°. The resulting powder diffraction patterns were analyzed according to the Joint Committee on Powder Diffraction Standard (JCPDS) data.

Batch sorption experiments

The factors determining the reduction and adsorption of Cr(VI) by nZVIs were investigated using batch sorption experiments including the ratio of solid to solution, the initial pH, and the initial chromium concentration. All batch experiments were conducted in 250 ml flasks in triplicate and stirred at 100 rpm for 18 hours at a constant temperature of 20 °C. The preliminary experimental result showed that 18 hours was sufficient for chromium reduction and adsorption to reach equilibrium. At the end of the batch experiments, each flask was centrifuged for 30 min at $3{,}000 \times$ g to separate the solid phase from the solution. Thereafter, the solids were freeze-dried for characterization of nZVI, and the supernatants were used to determine the concentration of total Cr using an atomic absorption spectrophotometer (PE AA800) and Cr(VI) using the 1.5-diphenylcarbohydrazide method (spectrophotometry).

RESULTS

Characterization of nZVIs

SEM

The morphologies of the two nZVIs are shown in Figure 1. It is evident that the two nZVIs were both spherical particles loaded on the carriers. Figure 1(a) shows that S-nZVI adhered to the starch chain uniformly, while C-nZVI was loaded on the surface of some kind of spherical particle, with obvious aggregation. To calculate the particle size distribution, 250 particles were selected randomly and the results showed that the size range of S-nZVI was 27.51–126.78 nm, with a mean of 62.56 nm, and the size distribution of C-nZVI was 30.89–187.2 nm, with a mean of 80.13 nm. Thus the particle size of S-nZVI was smaller and had a more uniform size distribution than C-nZVI.

XRD

The XRD spectra of the two nZVIs are presented in Figure 2. It can be seen that for S-nZVI the typical diffraction peaks of Fe^0 were at 44.7°–44.8°, with the satellite peaks of 65.0° and 82.3° (Dong *et al.* 2017). Similarly to S-nZVI, the pattern for C-nZVI showed that the main component of the particle was Fe^0, with the peak at 44.7° and satellite peak of 82°. The mean particle size was calculated as 40.35 nm for S-nZVI and 73.97 nm for C-nZVI, respectively, which were similar to the SEM results.

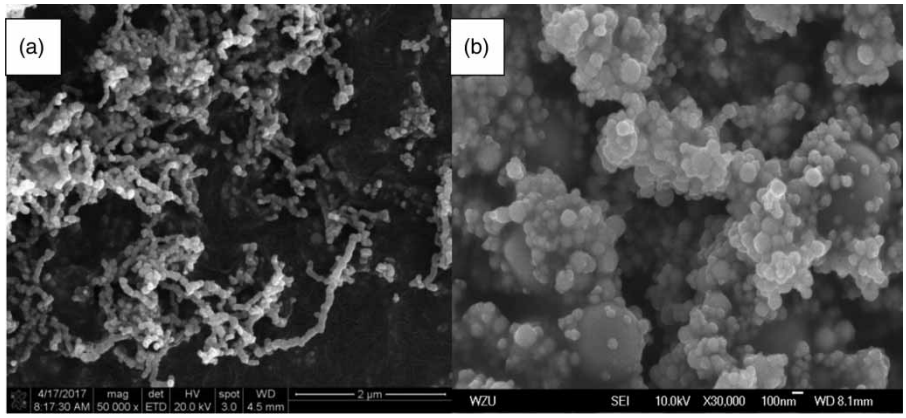

Figure 1 | Scanning electron microscopy (SEM) images of starch-stabilized nanoscale zero-valent iron (S-nZVI) and commercial nanoscale zero-valent iron (C-nZVI). (a) S-nZVI; (b) C-nZVI.

XPS

Panoramic XPS tests were conducted to detect the chemical compositions of the two nZVIs (Figure 3). From the survey spectra of S-nZVI, Fe, O and Na were identified, with less B and C. The predominant B 1 s peaks (narrow) were located at around 198 eV, indicating that $NaBH_4$ was not completely washed out. It was not surprising that C 1 s peaks at around 284.9 eV were found, suggesting the existence of a starch chain. Besides Fe and O, K was also observed in C-nZVI, along with less Na, Si, Mg, Ca and C, which may have been due to the composition of the nZVI carrier.

The narrow XPS test for Fe 2P showed a predominant peak at 715.8 eV, indicating the existence of Fe^{2+} in S-nZVI (Yamashita & Hayes 2008). Furthermore, the co-existence of Fe^{2+} and Fe^{3+} was identified based on the calculation of the binding energy at 710.2 eV and 712.0 eV for Fe $2P_{3/2}$. The relative contents of Fe^{2+} and Fe^{3+} calculated based on the area of the peaks were 33.33% and 66.67%, respectively. The main chemical forms of Fe were FeO at 710.2 eV and FeOOH at 712.0 eV. A small satellite peak at 706.1 eV was identified as the Fe^0 (Sun *et al.* 2007). The small shoulder peak at 719.4 eV was caused by the overlaid iron oxide ($2P_{3/2}$) and zero-valent iron ($2P_{1/2}$) (Li & Zhang 2007). Similarly, the shoulder peak at 715.4 eV for C-nZVI showed the existence of Fe^{2+}, and the calculated results (based on the area of the peaks of 710.2 eV and 711.5 eV) showed the relative contents of 28.5% Fe^{2+} and 71.5% Fe^{3+}. The chemical forms of Fe were identified as FeO at 710.2 eV, FeOOH at 711.5 eV and Fe^0 at 706.7 eV.

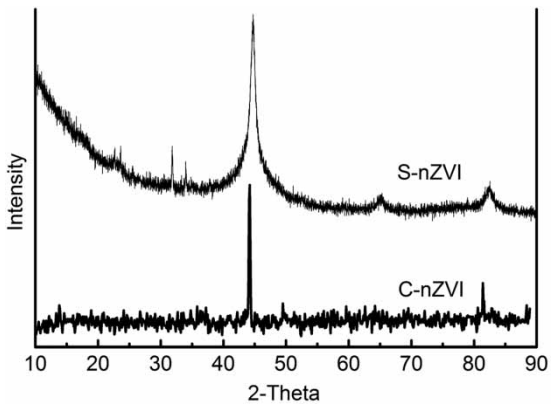

Figure 2 | X-ray diffraction (XRD) patterns of starch-stabilized nanoscale zero-valent iron (S-nZVI) and commercial nanoscale zero-valent iron (C-nZVI).

The effect of nZVI dosage on chromium removal

Chromium removal by the two nZVIs is presented in Figure 4, which shows that the removal efficiency of total Cr and Cr(VI) increased with the amount of nZVI added to the solution; however, the removal efficiencies of the two nZVIs differed. It is obvious that the removal efficiency of S-nZVI was higher than that of C-nZVI. For example, when the amount of nZVI was 0.2 g L^{-1}, the removal efficiencies of total Cr and Cr(VI) by S-nZVI were 74.37% and 73.90%, respectively, while the removal efficiencies by C-nZVI were 17.35% and 18.6%, respectively. When the amount of S-nZVI increased to 1.0 g L^{-1}, the removal efficiencies of total Cr and Cr(VI) approached 100%, whereas when the amount of C-nZVI increased to 6.0 g L^{-1}, the removal efficiencies of total Cr and Cr(VI) increased to 44.3% and 51.0%, respectively. Clearly, the removal ability of S-nZVI was much stronger than that of C-nZVI, which may have been due to its smaller particle size and the fact that it was less aggregated.

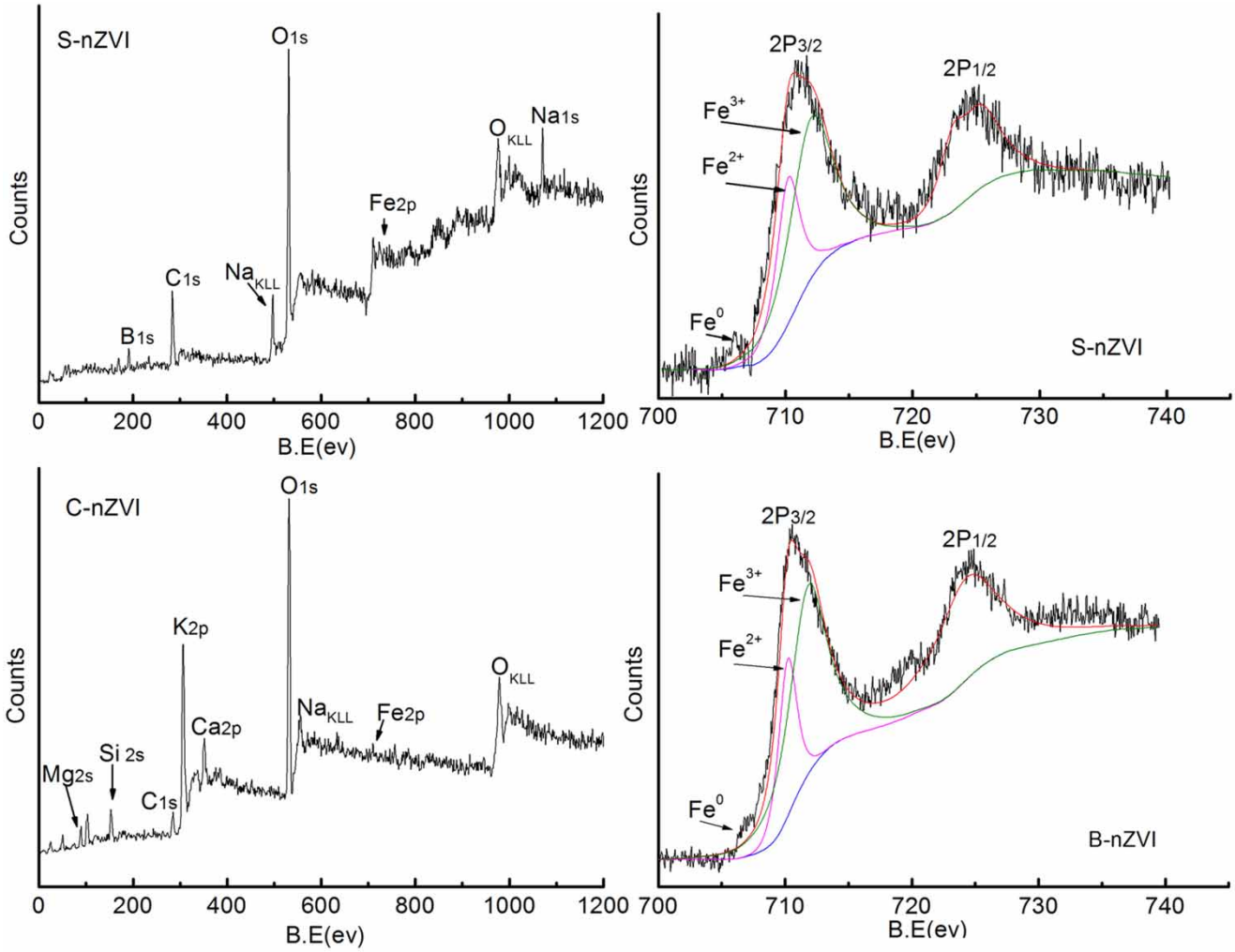

Figure 3 | X-ray photoelectron spectroscopy (XPS) images of starch-stabilized nanoscale zero-valent iron (S-nZVI) and commercial nanoscale zero-valent iron (C-nZVI).

The effect of pH on chromium removal by nZVI

pH is another important factor affecting the chromium removal efficiency by nZVI (Figure 5). For Cr(VI) reduction, it was unsurprising that low pH was advantageous since H^+ is necessary for reducing Cr(VI) to Cr(III). However, it was unexpected that a high efficiency of Cr(VI) reduction by S-nZVI occurred in a wide pH range (1–11). The same trend

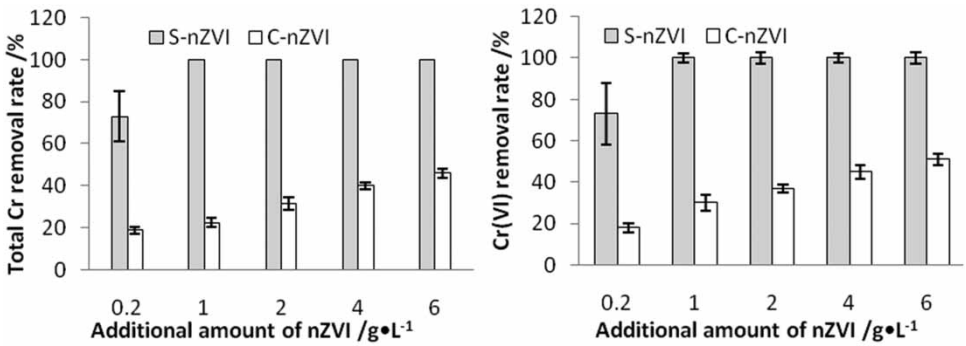

Figure 4 | Effect of different dosages of starch-stabilized nanoscale zero-valent iron (S-nZVI) and commercial nanoscale zero-valent iron (C-nZVI) on the removal efficiency of Cr(VI) and Cr_{total}.

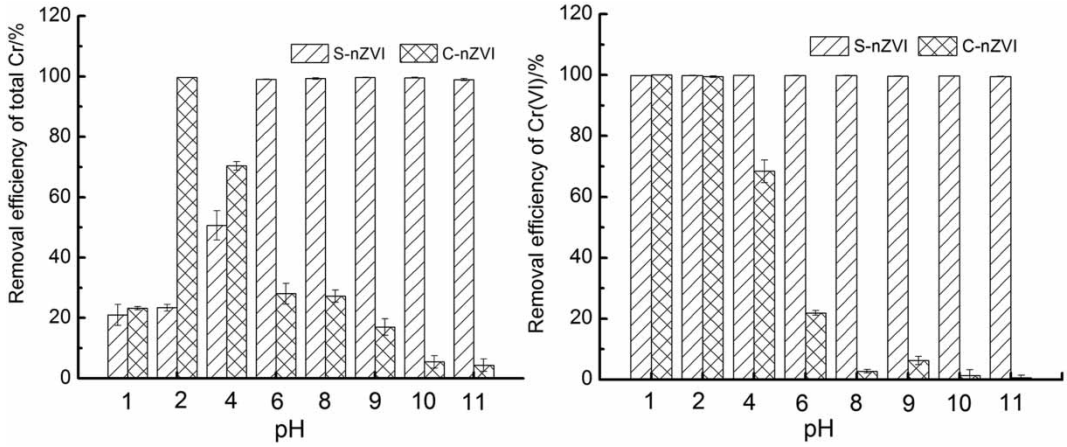

Figure 5 | Effect of different pH on the removal efficiency of Cr(VI) and Cr_{total}.

was observed for total Cr removal. The highest removal efficiency of total Cr by C-nZVI occurred at pH 2.0, while that for S-nZVI occurred at pH 6.0. The removal efficiency of total Cr by C-nZVI increased from pH 1.0 to pH 2.0, and then decreased gradually from pH 2.0 to pH 11.0. However, the removal efficiency of total Cr by S-nZVI increased to almost 100% from pH 1.0 to pH 6.0, and thereafter remained close to 100%. The obvious difference in chromium removal for the two nZVIs indicated the different removal mechanisms for total Cr and Cr(VI). The removal of total Cr by nZVI was due to Cr(VI) adsorption and Cr(III) precipitation on the surface of nZVI. In a low pH range, the high H^+ concentration of accelerated the reduction of Cr(VI) to Cr(III) but prevented the precipitation of Cr(III) onto the nZVI. With the increase in pH, OH^- competed with Cr(VI) (CrO_4^{2-}) for the sorption sites on the surface of nZVI, which decreased the removal of total Cr by C-nZVI. However, such a trend did not exist for S-nZVI, which may have been due to the high reduction of Cr(VI) to Cr(III) at pH 1–11.

Binding mechanism of chromium with nZVI

The XPS results of Cr2P and O1 s of nZVI after chromium adsorption are shown in Figure 6. From Figure 6, Cr $2P_{3/2}$ and $Cr2P_{1/2}$ were identified at the peaks of 577.3 eV and 587.5 eV, indicating the existence of Cr(III) in S-nZVI. Similarly, the peaks at 577.8 eV and 587.6 eV representing Cr(III) were found in C-nZVI. The Cr(VI) peaks at 579.8 eV for $Cr2P_{3/2}$ and 590.1 eV for $Cr2P_{1/2}$ were found in C-nZVI, whereas no Cr(VI) was evident in S-nZVI, which means that Cr(VI) was reduced to Cr(III) completely in S-nZVI, while 6.33% Cr(VI) of total Cr was found in C-nZVI, indicating that along with Cr(III), Cr(VI) could be adsorbed onto the surface of nZVI.

To determine the binding form of chromium in nZVI, the XPS of O was analyzed based on Figure 6, where it can been seen that O1 s XPS for both nZVIs was separated into three peaks of 530.1 eV, 531.5 eV and 532.5 eV, which represents the species of O^{2-}, OH^- and chemically combined water, respectively. The result indicated that chromium adsorbed onto the surface of nZVI existed in the form of $(Cr_xFe_{1-x})(OH)_3$ or $Cr_xFe_{1-x}OOH$ (Li & Zhang 2007). Similarly, Geng *et al.* (2009) reported that the passivation layer of hydroxide of $Cr_{0.667}Fe_{0.333}OOH$ or $(Cr_{0.667}Fe_{0.333})$ $(OH)_3$ on the surface of nanoparticle iron can prevent the oxidation of inner zero-valent iron in the particle. OH^- was calculated to be approximately 81.65% in S-nZVI and 24.8% in C-nZVI, indicating that oxygen was mainly in the form of OH^-, which easily adsorbs Cr^{3+} to form the membrane of Cr-Fe.

DISCUSSION

Two processes took place resulting in the removal of chromium by nZVI from the aqueous phase: chromium adsorption onto the nZVI particles and the reduction of Cr(VI) to Cr(III). The main speciation of Cr(VI) in solution is $HCrO_4^-$ in the range of pH 1–6 and CrO_4^{2-} when the pH is higher than 6 (Fu *et al.* 2017). Figure 6 shows that most Cr(VI) was initially reduced to Cr(III) by nZVI, and was then adsorbed onto the surface of nZVI. The process of

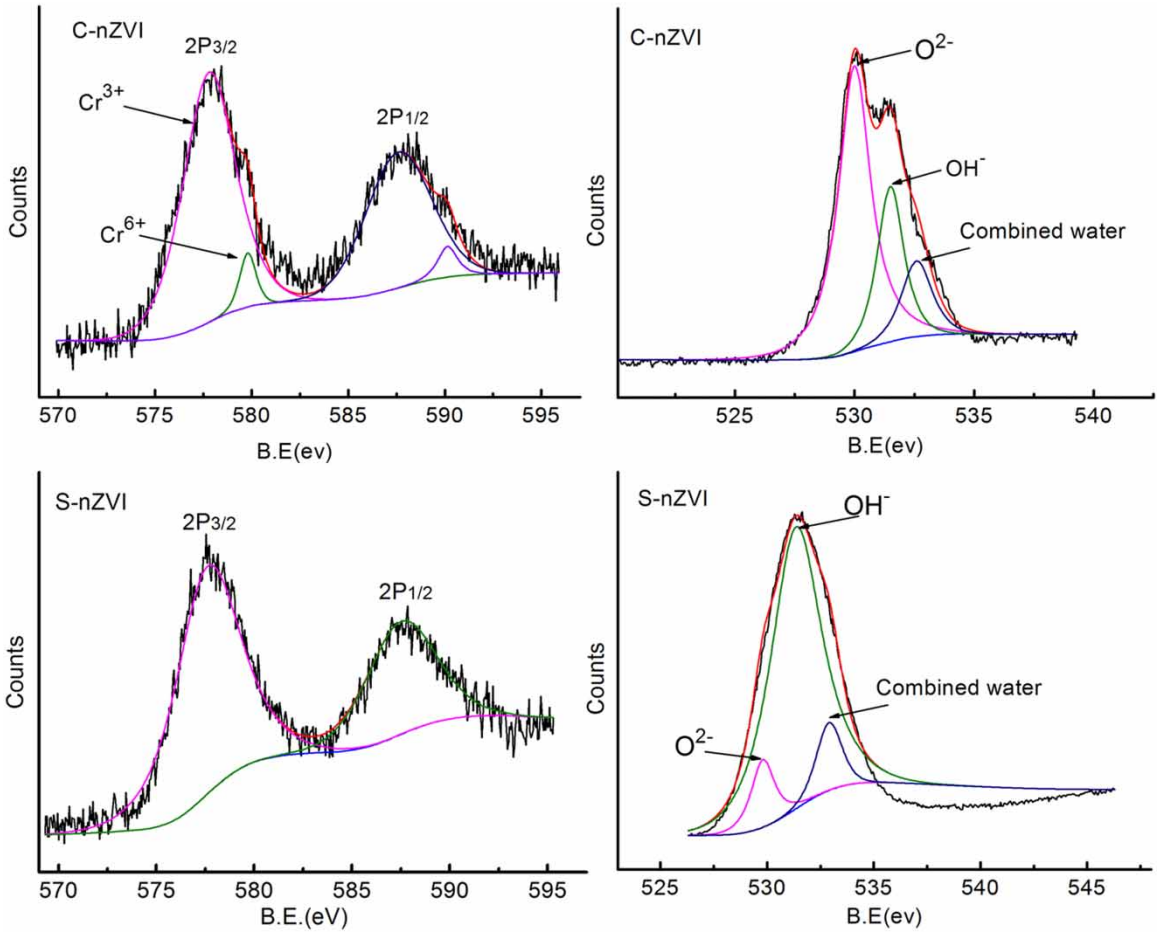

Figure 6 | Cr2P and O1 s XPS spectra of nanoscale zero-valent iron (nZVI) after Cr(VI) adsorption.

reduction was affected mainly by pH, following the reactions below (Zhou *et al.* 2015).

$$2HCrO_4^- + 3Fe^0 + 14H^+ \rightarrow 3Fe^{2+} + 2Cr^{3+} + 8H_2O \quad (1)$$

$$HCrO_4^- + 3Fe^{2+} + 7H^+ \rightarrow 3Fe^{3+} + Cr^{3+} + 4H_2O \quad (2)$$

According to Equations (1) and (2), it is obvious that a low pH can accelerate the reactions, which is supported by the results presented in Figure 5. However, excess H^+ will cause corrosion of iron particles. Except for the reduction by nZVI, adsorption of Cr(VI) by nZVI is another means of removing Cr(VI) from an aqueous medium. Actually, chromium (Cr^{3+} or CrO_4^{2-}) was adsorbed not only by nZVI but also by ferric hydroxide precipitation. As shown in Equations (1) and (2), Fe^0 was oxidized by Cr(VI) to Fe^{2+} and Fe^{3+}, inducing ferric hydroxide precipitation, as shown by the reaction in Equation (3).

$$Fe^{3+} + 3OH^- \rightarrow Fe(OH)_3 \quad (3)$$

The precipitate $Fe(OH)_3$ rapidly becomes FeOOH by dewatering as shown in Equation (4) (Li & Zhang 2007).

$$Fe(OH)_3 \rightarrow FeOOH + H_2O \quad (4)$$

When precipitation occurs, chromium may bind to ferric hydroxide by co-precipitation to form Cr-Fe hydroxide, such as $(Cr_xFe_{1-x})(OH)_3$ or $Cr_xFe_{1-x}OOH$.

Our results based on XRD and XPS analyses confirmed the core-shell structure of nZVI. The nZVI core was coated by ferric oxide, and the ferric oxide shell can prevent the oxidation of nZVI. The core-shell structure of nZVI is, therefore, beneficial for the removal of other metals from an aqueous medium. Our data on real wastewater suggested

Table 2 | Removal efficiency of heavy metals in electroplating wastewater by nanoscale zero-valent iron (nZVI)

		Removal efficiency (%)							
Element	Initial concentration (mg L^{-1})	C-nZVI				S-nZVI			
Amount of nZVI/g L^{-1}	–	2	5	10	20	2	5	10	20
Total Cr	712.20	48.56	60.20	95.26	99.89	69.97	93.26	100	100
Cr(VI)	510.81	60.36	96.46	99.87	100	61.97	98.03	100	100
Cu	138.10	36.86	63.32	82.62	97.55	49.46	93.03	98.64	99.77
Zn	318.40	11.73	49.69	76.74	82.26	31.01	51.24	96.71	100
Pb	5.76	100	100	100	100	100	100	100	100
Cd	0.96	100	100	100	100	100	100	100	100

the feasibility of nZVI for removing metals from wastewater (Table 2).

CONCLUSION

In summary, this study showed that starch-stabilized nanoscale zero-valent iron (S-nZVI) can efficiently remove Cr(VI) from the aqueous phase. Even in a wide pH range (1–11), S-nZVI removed almost 100% of Cr(VI), which was due to the strong reduction ability of S-nZVI in relation to Cr(VI). A small portion of Cr(VI) was directly adsorbed by S-nZVI, but the majority was removed by reduction to Cr^{3+} by S-nZVI and subsequent precipitation as $Cr(OH)_3$. The precipitated Cr^{3+} was bound to ferric hydroxide by co-precipitation to form Cr-Fe hydroxide, such as $(Cr_xFe_{1-x})(OH)_3$ or $Cr_xFe_{1-x}OOH$. The core-shell structure of nZVI is not only beneficial for Cr removal, but also for Cu, Zn, Pb, Cd removal from electroplating wastewater. Therefore starch-stabilized nanoscale zero-valent iron provides a valuable alternative as an efficient and magnetically separable adsorbent for Cr(VI) removal from contaminated wastewater.

ACKNOWLEDGEMENTS

The authors wish to thank the Zhejiang Natural Science Foundation of China (ZJNSF, Project No. LY17D010003), Science and Technology Department of Zhejiang Province (Project 2019C54002), Wenzhou Science and Technology Bureau (Project No. S20160002) for their partial funding support of this study.

REFERENCES

Ambika, S., Nambi, I. M. & Senthilnathan, J. 2016 Low temperature synthesis of highly stable and reusable CMC-Fe^{2+} (-nZVI) catalyst for the elimination of organic pollutants. *Chemical Engineering Journal* **289**, 544–553.

Broujeni, B. R., Nilchi, A., Hassani, A. H. & Saberi, R. 2018 Preparation and characterization of chitosan/Fe_2O_3 nano composite for the adsorption of thorium (IV) ion from aqueous solution. *Water Science & Technology* **78** (3), 708–720. http://doi: 10.2166/wst.2018.343.

Cao, H. S. & Zhang, W. X. 2006 Stabilization of chromium ore processing residue (COPR) with nanoscale iron particles. *Journal of Hazardous Materials* **132** (2), 213–219.

Chen, H. L., Arocena, J. M., Li, J. B., Thring, R. W. & Zhou, J. M. 2014 Assessments of chromium (and other metals) in vegetables and potential bio-accumulations in humans living in areas affected by tannery waste. *Chemosphere* **112**, 412–419.

Dong, J., Ren, L. M., Chi, Z. F. & Hu, W. H. 2017 Analysis of XPS in the removal of Cr(VI) from groundwater with *r*GO-nZ. *Spectroscopy and Spectral Analysis* **37** (1), 250–255.

Fu, R. B., Zhang, X., Xu, Z., Guo, X. P., Bi, D. S. & Zhang, W. 2017 Fast and highly efficient removal of chromium (VI) using humus-supported nanoscale zero-valent iron: influencing factors, kinetics and mechanism. *Separation and Purification Technology* **174**, 362–371.

Geng, B., Jin, Z. H., Li, T. L. & Qi, X. H. 2009 Kinetics of hexavalent chromium removal from water by chitosan-Fe^0 nanoparticles. *Chemosphere* **75** (6), 825–830.

Gheju, M. & Balcu, I. 2011 Removal of chromium from Cr(VI) polluted wastewaters by reduction with scrap iron and subsequent precipitation of resulted cations. *Journal of Hazardous Materials* **196**, 131–138.

Jabeen, H., Kemp, K. C. & Chandra, V. 2013 Synthesis of nano zero valent iron nanoparticles-graphene composite for the treatment of lead contaminated water. *Journal of Environmental Management* **130**, 429–435.

Klimkova, S., Cernik, M., Lacinova, L., Filip, J., Jancik, D. & Zboril, R. 2011 Zero-valent iron nanoparticles in treatment of acid mine water from in situ uranium leaching. *Chemosphere* **82**, 1178–1184.

Kong, X. K., Han, Z. T., Zhang, W., Song, L. & Li, H. 2016 Synthesis of zeolite-supported microscale zero-valent iron for the removal of Cr^{6+} and Cd^{2+} from aqueous solution. *Journal of Environmental Management* **169**, 84–90.

Kumarathilaka, P., Jayaweera, V., Wijesekara, H., Kottegoda, I. R. M., Rosa, S. R. D. & Vithanage, M. 2016 Insights into starch coated nanozero valent iron-graphene composite for Cr(VI) removal from aqueous medium. *Journal of Nanomaterials*. http://dx.doi.org/10.1155/2016/2813289.

Li, X. Q. & Zhang, W. X. 2007 Sequestration of metal cations with zerovalent iron nanoparticles-a study with high resolution X-ray photoelectron spectroscopy (HR-XPS). *Journal of Physical Chemistry C* **111** (19), 6939–6946.

Li, J., Chen, C. L., Zhu, K. R. & Wang, X. K. 2015 Nanoscale zero-valent iron particles modified on reduced graphene oxides using a plasma technique for Cd(II) removal. *Journal of the Taiwan Institute of Chemical Engineers* **59**, 389–394.

Mihaileanu, R. G., Neamtiu, I. A., Fleming, M., Pop, C., Bloom, M. S., Roba, C., Surcel, M., Stamatian, F. & Gurzau, E. 2019 Assessment of heavy metals (total chromium, lead, and manganese) contamination of residential soil and homegrown vegetables near a former chemical manufacturing facility in Tarnaveni, Romania. *Environmental Monitoring and Assessment* **191** (8), 1–13.

Nickens, K. P., Patierno, S. R. & Ceryak, S. 2010 Chromium genotoxicity: a double-edged sword. *Chemico-Biological Interaction* **188**, 276–288.

Sun, Y. P., Li, X. Q., Zhang, W. X. & Wang, H. P. 2007 A method for the preparation of stable dispersion of zero-valent iron nanoparticles. *Colloids and Surface A-Physicochemical And Engineering Aspects* **308** (1), 60–66.

Wang, C., Luo, H. J., Zhang, Z. L., Wu, Y., Zhang, J. & Chen, S. W. 2014 Removal of As(III) and As(V) from aqueous solutions using nanoscale zero valent iron-reduced graphite oxide modified composites. *Journal of Hazardous Materials* **268**, 124–131.

Wijesekara, S. S. R. M. D. H. R., Basnayake, B. F. A. & Vithanage, M. 2014 Organic-coated nanoparticulate zero valent iron for remediation of chemical oxygen demand (COD) and dissolved metals from tropical landfill leachate. *Environmental Science and Pollution Research* **21** (11), 7075–7087.

Yamashita, T. & Hayes, P. 2008 Analysis of XPS spectra of Fe^{2+} and Fe^{3+} ions in oxide materials. *Applied Surface Science* **254** (8), 2441–2449.

Zhao, X., Liu, W., Cai, Z. Q., Han, B., Qian, T. W. & Zhao, D. Y. 2016 An overview of preparation and applications of stabilized zero-valent iron nanoparticles for soil and groundwater remediation. *Water Research* **100**, 245–266.

Zhou, X. B., Lv, B. H., Zhou, Z. M., Li, W. X. & Jing, G. H. 2015 Evaluation of highly active nanoscale zero-valent iron coupled with ultrasound for chromium(VI) removal. *Chemical Engineering Journal* **281**, 155–163.

Zhu, S. S., Huang, X. C., Wang, D. W., Wang, L. & Ma, F. 2018 Enhanced hexavalent chromium removal performance and stabilization by magnetic iron nanoparticles assisted biochar in aqueous solution: mechanisms and application potential. *Chemosphere* **207**, 50–59.

First received 19 June 2019; accepted in revised form 10 October 2019. Available online 29 October 2019